Mechanism of Phenylalanyl-tRNA Synthetase of *Escherichia coli* K 10. Modulation of Catalytic Properties by Magnesium†

Jutta Pimmer and Eggehard Holler*

ABSTRACT: The association of phenylalanyl-tRNA and Mg^{2+} follows a biphasic concentration dependence as indicated by the active site directed fluorescent indicator 2-*p*-toluidinylnaphthalene-6-sulfonate. The macroscopic dissociation constants are 0.16 ± 0.03 and 4.1 ± 0.5 mM. The effect of Mg^{2+} on the association of enzyme and MgATP, on the synergistic binding of MgATP and L-phenylalaninol, and on the pre-steady-state synthesis and pyrophosphorolysis of the enzyme·phenylalanyladenylate complex in the absence and the presence of $tRNA^{Phe}$ has been measured by established equilibrium and stopped-flow techniques using 2-*p*-toluidinylnaphthalene-6-sulfonate. At 10 mM Mg^{2+}, the association of enzyme and MgATP is biphasic with dissociation constants of 0.25 ± 0.03 and 9.1 ± 1.7 mM. At 2 mM Mg^{2+}, a single dissociation constant of 5.0 ± 0.5 mM is indicated. The coupling constant of the synergistic reaction is 15 at 1 mM Mg^{2+} and 290 at 10 mM Mg^{2+}. The Hill constant of the sigmoidal dependence is 3.6. The strengthening of the synergism is believed to reflect a Mg^{2+}-dependent coupling of the synergistic reactions at the two active sites of the enzyme, the coupling being negligible at 1 mM and maximal at 10 mM Mg^{2+}. The pre-steady-state rate of adenylate synthesis is accelerated by the presence of Mg^{2+}. The effect is to decrease the value of the Michaelis–Menten constant of MgATP. Another effect is to increase the rate constant when $tRNA^{Phe}$ is present. At subsaturating [MgATP], the [Mg^{2+}] dependence of the observed rate constant is hyperbolical in the absence and sigmoidal (Hill constant, 3.5) in the presence of $tRNA^{Phe}$. The rate of the pyrophosphorolysis is enhanced by a decrease of the Michaelis–Menten constant of $MgPP_i$. The effects on the thermodynamics and kinetics parallel the occupancy of the low-affinity Mg^{2+}-binding sites of the enzyme.

Magesium ions are known to be required as cofactors during the aminoacylation of tRNA as catalyzed by the aminoacyl-tRNA synthetases. Their general function is to chelate with ATP, which only in this form is active as a substrate (Cole & Schimmel, 1970). Additional magnesium is necessary to achieve maximum enzymatic activity. This is because the cation associates with the synthetase and with the transfer ribonucleic acid. While the cation requirement of native tRNA has been generally accepted, there are only a few examples for the need to associate with the synthetases (Craine & Peterkofsky, 1976; Bartmann et al., 1975a; Holler, 1976). In the present publication, we have focused on the question whether magnesium is capable of modulating the ligand binding properties and catalytic rates of phenylalanyl-tRNA synthetase.

Materials and Methods

L-Phenylalanyl-tRNA synthetase (EC 6.1.1.20) was prepared from *Escherichia coli* K 10 in the presence of phenylmethanesulfonyl fluoride as described by Hanke et al. (1974). Specific activity was 15000 nmol of aminoacyl-tRNA mg^{-1} h^{-1} and 1.95 active sites per enzyme (molecular weight 270000). Inorganic pyrophosphatase (EC 3.6.1.1) from yeast was obtained from Boehringer (Mannheim) in the form of a 1 mg/mL (200 U/mg) suspension in 3.2 M ammonium sulfate. $tRNA^{Phe}$ having an amino acid acceptance of 1200 pmol per A_{260} unit (at pH 7 in H_2O) was purchased from Boehringer. Enzyme activity and tRNA charging capacity were measured as described by Kosakowski & Böck (1970). Complete charging was achieved by using comparable amounts of tRNA and synthetase. The charging was routinely followed over a time period of 20 min. The number of active sites was established by the filter assays described previously (Bartmann et al., 1975a; Rainey et al., 1977).

Uniformly labeled L-[^{14}C]phenylalanine with a specific radioactivity of 350–500 Ci/mol was obtained from Radiochemical Centre (Amersham). TNS[1] was purchased from Serva (Heidelberg) and ATP from Boehringer (Mannheim). L-Phenylalaninol was from Fluka (Buchs) and has been analyzed for homogeneity as described (Kosakowski & Holler, 1973). α,β-Methyleneadenosine triphosphate from Miles was chemically homogeneous according to chromatography on polyethylenimine–cellulose thin-layer sheets, Polygram Cel-300 from Machery and Nagel/Düren (Goody & Eckstein, 1971). All other chemicals (analytical grade) were from Merck (Darmstadt).

In most experiments, the buffer contained 50 mM Tris-HCl (pH 7.5), 0.1 mM EDTA, and 0.2 mM dithioerythritol.

Equilibrium Fluorescence Measurements. Dissociation constants were determined for the binding of ligands by titration of the highly fluorescent synthetase·TNS complex as has been described (Kosakowski & Holler, 1973; Bartmann et al., 1975a). A Perkin-Elmer MPF-2A fluorescence spectrophotometer thermostated at 25 ± 0.5 °C and 4 × 10 mm quartz cuvettes (excitation light entered the narrow side) from Hellma (Müllheim) were used.

Circular Dichroism. Spectra were obtained by using a Roussel-Jouan Dichrographe II with scale expansion (ΔE = 2×10^{-6}/mm). Cuvettes with 5-mm pathlength were used. The sample absorbance was 0.75.

Kinetic Measurements. Kinetics were followed by the observation of the time-dependent decrease of the fluorescence intensity concomitant with the displacement of TNS from the phenylalanine-specific binding site of the synthetase (Kosakowski & Holler, 1973). Rapid mixing of the reactants was performed with a Durrum-Gibson stopped-flow spectropho-

† From the Fachbereich Biologie und Vorklinikum, Universität Regensburg, D-8400, Federal Republic of Germany. *Received May 3, 1978; revised manuscript received April 24, 1979.* The work was generously supported by the Deutsche Forschungsgemeinschaft and the Fonds der Chemischen Industrie.

[1] Abbreviations used: TNS, 2-*p*-toluidinylnaphthalene-6-sulfonate; APCPP, α,β-methyleneadenosine triphosphate; Tris, 2-amino-2-hydroxymethyl-1,3-propanediol; EDTA, (ethylenedinitrilo)tetraacetic acid.

0006-2960/79/0418-3714$01.00/0

tometer with fluorescence equipment as described (Rainey et al., 1977; Bartmann et al., 1975a). Both drive syringes contained TNS, buffer, and $MgCl_2$ at identical concentrations.

The progress of the change in the fluorescence intensity was recorded on a Tektronix 7623A storage oscilloscope by using a 7A18 dual trace amplifier and a 7B53A dual time base unit. The stored oscilloscope traces were photographed and evaluated as first-order kinetics. In all cases, the time dependence could be fitted within 80–90% of the total change in the fluorescence intensity by a single exponential. The obtained values of the first-order rate constants were analyzed as a function of the concentrations of reactants according to eq 1

$$k_{obsd} = k_f \frac{[Phe]_0[MgATP]_0}{([Phe]_0 + K_{Phe})([MgATP]_0 + K_{MgATP})} + k_b \frac{[MgPP_i]_0}{K_{MgPP_i}^{Phe\sim AMP} + [MgPP_i]_0} \quad (1)$$

as has been described previously (Holler & Calvin, 1972; Bartmann et al., 1975a; Hyafil & Blanquet, 1977). The various symbols are defined by eq 2. Equation 1 is an approximation because of the following assumptions. (a) The formation of the complexes from free reactants is in preequilibrium with the synthesis of the adenylate. (b) The formation of the ternary enzyme·substrate complex is described by the dissociation constants of the binary complexes, $K_{Phe} = K_{Phe}^{MgATP}$ and $K_{MgATP} = K_{MgATP}^{Phe}$. (c) The concentration of accumulating free $MgPP_i$ is low in order to neglect the competition between MgATP and $MgPP_i$ for associating with the enzyme. (d) Substrates are in excess over the synthetase so that initial concentrations can be used. (e) The observed decrease of the fluorescence intensity can be correlated with the synthesis of E·Phe~AMP, which does not dissociate during the time elapsing for the measurement.

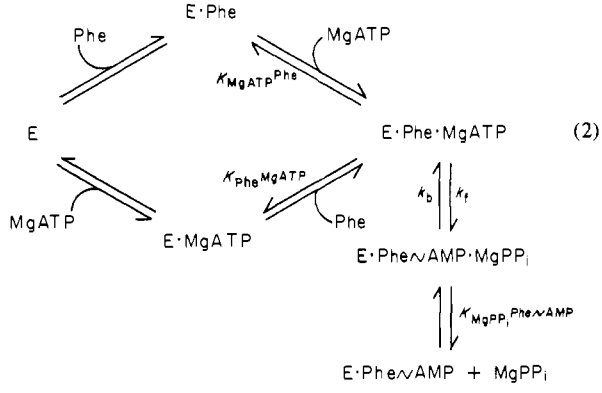

Assumptions a and b would be justified, for instance, if the observed values of the Michaelis–Menten constants, $K_{m(MgATP)}$, $K_{m(Phe)}$, and $K_{m(MgPP_i)}$, were identical with the values of the dissociation constants for the binary complexes. In any other case, the overall form of eq 1 is tentatively maintained and the symbols for the dissociation constants are replaced by those for the Michaelis–Menten constants. We shall refer to these in the Results. Assumptions c and d can be satisfied by the choice of appropriate concentrations. Assumption e is likely to be valid if the complexes E·Phe and E·MgATP·nMg^{2+} form and dissociate considerably faster than the intermediate is synthesized. Results of control experiments were in accord with this assumption.

Equation 1 is further simplified by neglecting the term for the reverse reaction. Similarly, the formation of the adenylate (in eq 1, the term containing the rate constant k_f) is omitted when the reverse reaction is investigated. This simplification

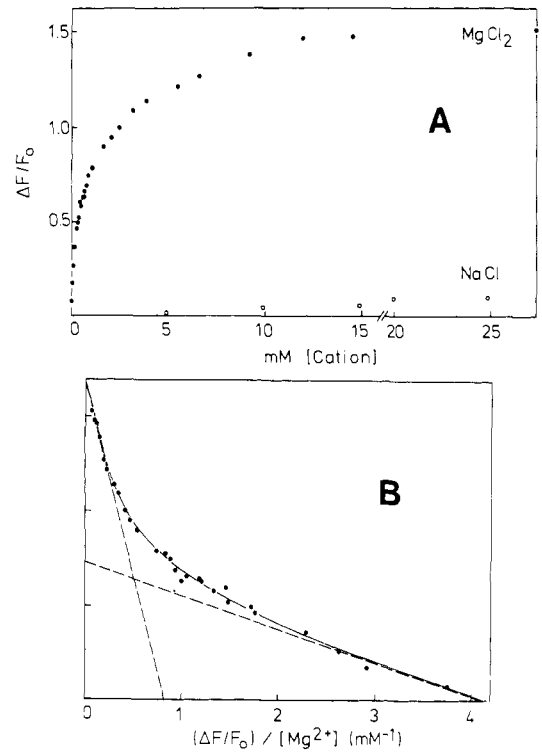

FIGURE 1: Titration of the enzyme·TNS complex with $MgCl_2$. Observation of the increase in fluorescence intensity. The reaction mixture contains 50 mM Tris-HCl buffer (pH 7.5 at 25 °C), 0.02 mM EDTA, 0.2 mM dithioerythritol, 8 μM TNS, and 0.4 μM phenylalanyl-tRNA synthetase. $MgCl_2$ is added with a 10-μL syringe in small quantities. The increase in intensity of the fluorescence emitted by the enzyme-bound TNS is given with respect to the initial intensity of the fluorescence F_0 (Mg^{2+} absent) and is plotted as a function of the Mg^{2+} concentration in A and according to the method of Eadie (1942) in B. The drawn curve is computed by use of the values of the microscopic dissociation constants and of the maximum fluorescence intensities given in Table I. The equation used is $\Delta F/F_0 = 0.66[Mg^{2+}]/(0.171 \times 10^{-3} + [Mg^{2+}]) + 1.01[Mg^{2+}]/(3.9 \times 10^{-3} + [Mg^{2+}])$ as has been suggested by Klotz & Hunston (1971). The tangents given in B are the best fit of the computed curve with the experimental points. The effect of NaCl on fluorescence intensity is given for comparison. The chelating effect of EDTA is taken into account by assuming that all EDTA was complexed to Mg^{2+} (K_{diss} = 1.6 μM; Lynch & Schimmel, 1974). The effective concentrations of Mg^{2+} and of Mn^{2+} are calculated as the difference between the total cation concentration and the concentration of EDTA.

holds as long as the concentrations of the substrates of the neglected reactions are low with respect to their dissociation constants. In the present case, the following limits were considered: $[MgATP] \leq 0.1K_{MgATP}$; $[Phe] \leq 0.1K_{Phe}$; $[MgPP_i] \leq 0.01K_{MgPP_i}^{Phe\sim AMP}$. Another crucial point requires that the values of k_f and k_b be of similar size. During synthesis of up to 1 μM adenylate, the presence of 5–10 μg/mL inorganic pyrophosphatase is sufficient to almost instantaneously hydrolyze the released pyrophosphate.

Results

Enzyme·Mg^{2+} Complexes. When a mixture of phenylalanyl-tRNA synthetase and TNS was titrated with Mg^{2+}, an increase of the intensity of the fluorescent light emitted by the dye is observed (Figure 1). This increase has been plotted as a function of the Mg^{2+} concentration by the method of Eadie (1942). The experimental points do not follow a linear relation as would have been expected for a single class of binding sites but indicate a biphasic dependence (Figure 1B). The simplest explanation was to assume two classes of binding sites. The dissociation constants which pertain to each class have been determined by the tangent method of Klotz &

Table I: Phenylalanyl-tRNA Synthetase Complexes of Mg^{2+}, Mn^{2+}, or Spermine Tetrahydrochloride as Detected by the Fluorescence of Enzyme-Bound TNS[a]

cation	$\Delta F_{\infty(1)}/F_0$	$\Delta F_{\infty(2)}/F_0$	dissoc constants (mM) 1	2
Mg^{2+}	0.5 ± 0.1	0.95 ± 0.20	0.17 ± 0.03 (0.16)	3.9 ± 0.5 (4.1)
Mn^{2+}	0.18 ± 0.05	0.64 ± 0.10	0.030 ± 0.002 (0.030)	4.5 ± 0.5 (4.5)
spermine^{4+}	0.26 ± 0.05	0.74 ± 0.10	0.005 ± 0.002 (0.005)	0.23 ± 0.10 (0.23)

[a] The evaluation of the parameters for Mg^{2+} is described in the text and is carried out in the same way for the other cations. Dissociation constants are microscopic or macroscopic (in parentheses). Average errors are given with respect to three or four determinations. Conditions are 50 mM Tris-HCl buffer (pH 7.5 at 25 °C), 0.02 mM EDTA, 0.2 mM dithioerythritol, 2–13 μM enzyme, 0.02–28 mM $MgCl_2$, 0.006–10 mM $MnCl_2$, and 0.001–5 mM spermine hydrochloride.

Hunston (1971). The method is based on the assumption of independent binding sites. This model may not hold in the face of the results obtained for the substrates (Bartmann et al., 1975a), which suggest sequential binding and anticooperativity. At the present, the exact mechanism is unknown, and the true values of the individual dissociation constants cannot be assigned.

A set of microscopic dissociation constants was calculated according to Klotz & Hunston (1971) for each set of tangents drawn in Figure 1B. By using the constants, a curve was computed as shown in the figure. The best fit with the experimental points was obtained for the slopes 0.49 mM^{-1} and 6.0 mM^{-1}. The microscopic and macroscopic dissociation constants are given in Table I. The computation was based on the maximum degrees of the increase in fluorescence intensity corresponding to the occupation of the two classes of binding sites. $\Delta F_{\infty(1)}/F_0$ belongs to the high affinity sites and is obtained as the intercept of the tangent on the low concentration side (Figure 1B). $\Delta F_{\infty(2)}/F_0$ belongs to the low affinity sites. It is obtained from the intercept(2) of the tangent at the high concentration side according to $\Delta F_{\infty(2)}$ = intercept(2) − $\Delta F_{\infty(1)}/F_0$. The values are included in Table I.

Experiments with TNS concentrations varying between 2 μM and 13 μM gave very similar results. In another experiment, it was shown that the observed increase in fluorescence intensity cannot be attributed to an unspecific effect of the increase in ionic strength during the titration. The presence of NaCl from 0 to 125 mM in place of $MgCl_2$ revealed only a marginal increase of the fluorescence intensity following a linear concentration dependence (Figure 1).

$tRNA^{Phe}$ at 5 μM which almost saturates both binding sites (Bartmann et al., 1975a) had no effect on the results observed in its absence. Saturating concentrations of L-phenylalanine (10 mM) completely abolished the fluorescence effects of Mg^{2+}, whereas MgATP at 5 mM did not suppress the increase in fluorescence intensity completely.

Complexes of the Enzyme and Manganese(II) or Spermine. Manganese(II) and sperminium ions are generally known to replace Mg^{2+} in many biological reactions. Their ability to bind to phenylalanyl-tRNA synthetase and to increase the fluorescence intensity was found to be similar to that of Mg^{2+}. Again, biphasic concentration dependences were observed, the thermodynamical and fluorescence properties being summarized in Table I. For the three cations, the values of the dissociation constants of the two classes of binding sites are separated by factors between 25 for Mg^{2+} and 150 for Mn^{2+} and the ratios of $\Delta F_{\infty(2)}/F_0$:$\Delta F_{\infty(1)}/F_0$ to be in the range of 1.9 to 3.5. Spermine binds strongest followed by manganese(II). They probably occupy the same loci on the enzyme as may be concluded from an experiment in which a titration was performed with Mg^{2+} after the first binding site(s) had been (almost) saturated with spermine (15 μM). In this case, a monophasic titration curve was obtained for Mg^{2+} following the dissociation constant of 4.9 ± 1.0 mM.

A Search for Spectrophotometric Effects of Mg^{2+}. Circular dichroism of the enzyme was measured at zero, 1 mM, and 10 mM concentrations of Mg^{2+}. The synthetase was present at 2 mg/mL in Tris-HCl buffer (pH 7.5, 25 °C). An average of three runs was collected at each condition by using identical solutions and adding minute volumes of a Mg^{2+} stock solution (less than 0.5% v/v) or water to the sample and reference, respectively. The spectra (250–320 nm) were identical within experimental error.

Fluorescence spectra were measured for solutions which contained 0.15 μM phenylalanyl-tRNA synthetase and which were otherwise identical with those of the circular dichroism measurements. The emission spectra were recorded between 300 and 400 nm (with excitation at 290 nm) and the excitation spectra between 240 and 320 nm (with emission at 333 nm = maximum). Again, the spectra were found to be independent of Mg^{2+}.

Kinetics of Mg^{2+} Binding to the Enzyme·TNS Complex. Enzyme (0.16 μM) in a solution containing 50 mM Tris-HCl (pH 7.5), 0.4 mM dithioerythritol plus or minus 1 mM EDTA, and 9 μM TNS was mixed at 25 °C with 20 mM $MgCl_2$ in a solution containing the same ingredients except EDTA. A stopped-flow apparatus was used. An increase in fluorescence intensity was observed, 90% of which followed a single exponential decay with k_{obsd} = 206 ± 11 s^{-1} and 10% following a slow time dependence with k_{obsd} of approximately 0.7 s^{-1}. This slow dependence possibly reflects unspecific binding of TNS (other than at the phenylalanine-specific site) and was not further investigated. In an experiment using the same ingredients except that the enzyme solution contained 10 mM $MgCl_2$ instead of EDTA and the other solution 20 mM EDTA instead of $MgCl_2$, a decrease in intensity was observed consisting again of 90% which followed a k_{obsd} = 250 ± 30 s^{-1} and 10% a k_{obsd} of approximately 0.7 s^{-1}. In another experiment, the fluorescence was observed upon mixing the enzyme and varying amounts of L-phenylalanine. The decrease in fluorescence intensity was single exponential (k_{obsd} = 220 ± 20 s^{-1}) and the kinetics independent of the concentration of the amino acid. Similar results were obtained for the saturation of the enzyme with MgATP in solutions that contained 2–10 mM $MgCl_2$. Also, neither $MgPP_i$ (0.05–10 mM) nor $tRNA^{Phe}$ (0.01–20 μM) had an effect on the kinetics seen for the mixing of $MgCl_2$ and enzyme·TNS.

Enzyme·MgATP Complexes. The enzyme·TNS complex was titrated with MgATP in the presence of 2 mM and 10 mM $MgCl_2$, respectively. The essential conditions are given in Figure 2. The fluorescence intensity was observed to decrease in a monophasic (2 mM $MgCl_2$) and biphasic (10 mM $MgCl_2$) manner, respectively. The monophasic dependence covers the concentration range 0.1–10 mM MgATP. The values of the dissociation constants and of the maximum decrease for the MgATP-binding sites were calculated from the biphasic titration curve as described under Figure 1. As is seen in Figure 2, the calculated curve gives a rather poor fit to the experimental points for reasons that are not understood at the moment. In the case of the monophasic titration curve, the dissociation constant was calculated from

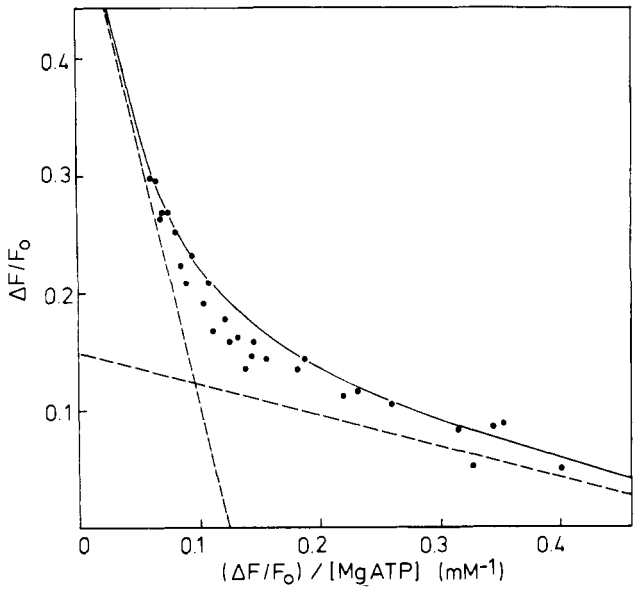

FIGURE 2: Linearized plot of the decrease in fluorescence intensity following the association of MgATP to enzyme·TNS in the presence of 10 mM Mg^{2+}. The biphasic binding of MgATP is evaluated according to the method described in Figure 1. The tangents and the drawn curve give the best fit to the experimental points. The equation used for the computation is $\Delta F/F_0 = 0.15[MgATP]/(0.26 \times 10^{-3} + [MgATP]) + 0.449[MgATP]/(8.8 \times 10^{-3} + [MgATP])$. ΔF refers to the decrease in fluorescence intensity at the concentration of MgATP added and F_0 the fluorescence intensity in the absence of MgATP. Conditions are 50 mM Tris-HCl buffer (pH 7.5 at 25 °C), 0.8 μM enzyme, 8 μM TNS, 0.02 mM EDTA, and 0.4 mM dithioerythritol. MgATP consists of equimolar solutions of $MgCl_2$ and ATP at pH 7.5.

Table II: Titration of Enzyme·TNS with MgATP[a]

Mg (mM)	$\Delta F_\infty/F_0$	slope (mM)	dissoc constant: microscopic (mM)	dissoc constant: macroscopic (mM)
2	0.30 ± 0.04	5.0 ± 0.5		5.0 ± 0.5
10	0.15 ± 0.02	0.26 ± 0.03	0.26 ± 0.03	0.25 ± 0.03
	0.45 ± 0.05	4.5 ± 0.7	8.8 ± 1.5	9.1 ± 1.7

[a] L-Phenylalanyl-tRNA synthetase was titrated as described for 10 mM Mg^{2+} under Figure 2. Plots of $\Delta F/F_0$ vs. $(\Delta F/F_0)[MgATP]^{-1}$ are monophasic at 2 mM and biphasic at 10 mM $MgCl_2$. For conditions other than $[Mg^{2+}]$, see Figure 2.

the slope of a $\Delta F/F_0$ vs. $\Delta F/F_0[MgATP]^{-1}$ plot (Holler et al., 1971). The results are listed in Table II.

Synergistic Enzyme Complexes of MgATP and L-*Phenylalaninol.* The formation of an enzyme·L-phenylalaninol complex is followed in the presence of TNS by measurement of the decrease in fluorescence intensity (Kosakowski & Holler, 1973). The amino alcohol binds to the site of L-phenylalanine, and the mechanism that leads to the observed decrease in intensity is probably the same as for the amino acid (Kosakowski & Holler, 1973). Enzyme·TNS was titrated with the amino alcohol at various constant concentrations of Mg^{2+}. The degree of the intensity decrease was plotted as a function of $\Delta F/$[phenylalaninol] according to the method applied in Figure 1. The dependence was linear in all cases. The dissociation constants were calculated from the slopes of the lines with the best fit to the experimental points. The competition between TNS and L-phenylalaninol leads to somewhat higher values for the apparent dissociation constants in comparison with the true values in the absence of the dye. The concentration of TNS was 4 μM; the dissociation constant of the enzyme·TNS complex is 0.069 mM at zero Mg^{2+} and 0.02 mM at 10 mM Mg^{2+} (Holler & Kosakowski, 1973). Since K_{diss}(app)/K_{diss}(true) = 1 + [TNS]/K_{diss}^{TNS}, the values calculated from the slopes are off by 6–20%. This deviation falls within the experimental error, and the values of the dissociation constants are given in Table III without correction.

Table III: Enzyme·L-Phenylalaninol Complexes at Various Concentrations of Mg^{2+} [a]

Mg^{2+} (mM)	0	1	2	3	5	7	12.5
K_{Pheol} (mM)	0.23[b]	0.22	0.22	0.31	0.53	0.86	1.2

[a] Experimental conditions are 50 mM Tris-HCl buffer (pH 7.5 at 25 °C), 0.02 mM EDTA, 4 mM dithioerythritol, 4 μM TNS, 0.4–0.8 μM phenylalanyl-tRNA synthetase, and 0.02–5 mM L-phenylalaninol. The fluorescence of TNS was measured in a Hitachi Perkin-Elmer MPF-2A fluorometer. [b] Holler et al., 1975.

The synergistic coupling is expressed as an enhancement of the affinity of either MgATP or L-phenylalaninol to form an enzyme complex when the other ligand is bound prior to this association (Kosakowski & Holler, 1973; Blanquet et al., 1975). Titrations were performed with L-phenylalaninol at various concentrations of MgATP and Mg^{2+}. Each binding curve, obtained as a decrease in fluorescence intensity of TNS at progressive concentrations of L-phenylalaninol, was evaluated by the method mentioned under Figure 1 to obtain the apparent dissociation constant of the enzyme·phenylalaninol complex, K_{Pheol}^{MgATP}(app). Since all plots of ΔF vs. $\Delta F/$[phenylalaninol] were linear with respect to the best fit of the experimental points, this constant was calculated directly from the various slopes.

The dissociation constant has been derived by Kosakowski & Holler (1973) to be related to the concentration of MgATP and the four dissociation constants defined in the reaction scheme (eq 3) by eq 4. The symbol $[MgATP]_0$ refers to the

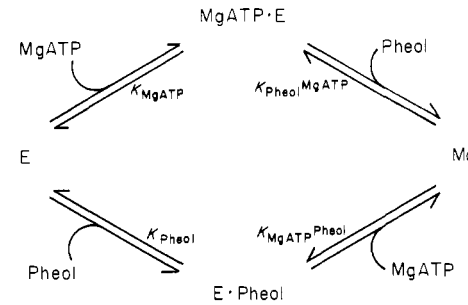

$$K_{Pheol}^{MgATP}(app) = K_{Pheol}\frac{K_{MgATP}^{Pheol}}{K_{MgATP}^{Pheol} + [MgATP]_0}\frac{K_{MgATP} + [MgATP]_0}{K_{MgATP}} \quad (4)$$

initial concentration of MgATP. In case the nucleotide concentration is high so that $[MgATP]_0 \gg K_{MgATP}^{Pheol}$, eq 4 is approximated by eq 5. The effect of one ligand on the

$$K_{Pheol}^{MgATP}(app) = \frac{K_{MgATP}^{Pheol}K_{Pheol}}{[MgATP]_0} + \frac{K_{Pheol}K_{MgATP}^{Pheol}}{K_{MgATP}} \quad (5)$$

dissociation constant of the other is defined as the coupling constant s (eq 6). The coupling constant was determined as

$$s = \frac{K_{MgATP}}{K_{MgATP}^{Pheol}} = \frac{K_{Pheol}}{K_{Pheol}^{MgATP}} \quad (6)$$

follows. The measured K_{Pheol}^{MgATP}(app) was plotted as a function of $[MgATP]_0^{-1}$ at conditions that led to the approximation eq 5 ($[MgATP]_0 \geq 0.2$ mM). The experimental points could be fit in all cases by linear approximations (not shown). With the known values for K_{Pheol}, the coupling

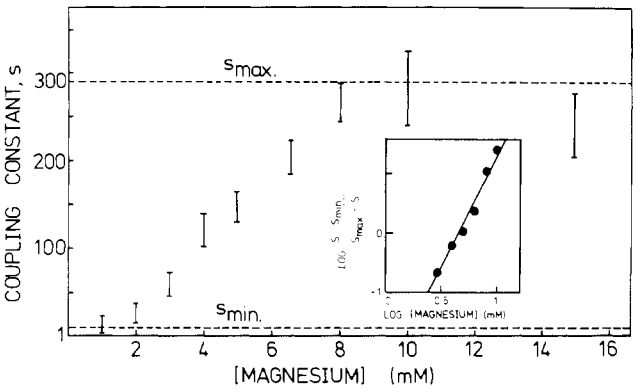

FIGURE 3: Effect of magnesium on the synergistic coupling constant. The coupling constant is computed as $s = K_{MgATP}/K_{MgATP}^{Pheol}$ from secondary plots as is described in the text. Experimental conditions are 50 mM Tris-HCl (pH 7.5 at 25 °C), 0.02 mM EDTA, 0.4 mM dithioerythritol, 0.4–0.8 μM phenylalanyl-tRNA synthetase, 4 μM TNS, 0.002–3 mM L-phenylalaninol, and 0.1–2 mM MgATP. The Hill plot in the figure inset is based on the equation $(s - s_{min})/(s_{max} - s_{min}) = [\text{magnesium}]^n/(K_{1/2} + [\text{magnesium}]^n)$, where n denotes the Hill constant (Hill, 1910) and $K_{1/2}$ the concentration of Mg^{2+} at $s_{max}/2$.

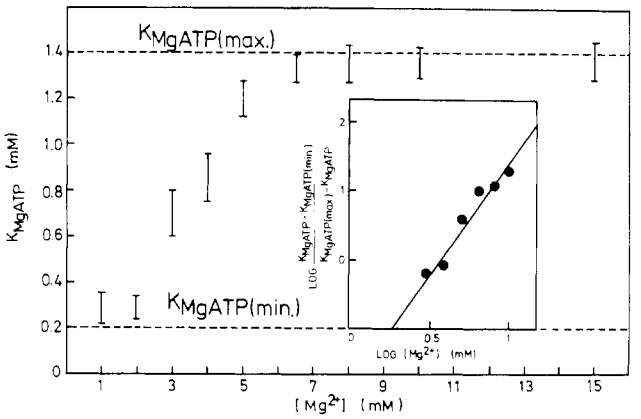

FIGURE 4: Effect of magnesium on the dissociation of the enzyme·MgATP complex as measured by the synergistic coupling phenomenon. The dissociation constant K_{MgATP} which functions in the synergistic coupling is computed from the slopes and intercepts of secondary plots according to eq 3 as described in the text. The synergistic partner is L-phenylalaninol (0.002–3 mM). The limiting values $K_{MgATP}(max)$ and $K_{MgATP}(min)$ were used to derive the Hill plot in the inset. As in Figure 3, the bars refer to the average scattering from three to five determinations. The experimental conditions are the same as in Figure 3.

constant was calculated from the intercept of the line which gave the best fit to the points. Equation 5 is also suitable to determine indirectly the dissociation constant of the binary enzyme·MgATP complex that functions in the synergistic coupling. For this purpose, the value of the slope was divided by the value of the intercept.

In Figure 3, the coupling constant, s, is plotted as a function of the magnesium concentration. The dependence is sigmoidal. At 1 mM Mg^{2+} the coupling constant is $s = 15$ and, at $\gtrsim 8$ mM, $s = 290$. The concentration of Mg^{2+} at $(s_{max} - s_{min})/2$ is 5 mM. The Hill constant from the double-logarithmic plot (Hill, 1910) in the figure inset is 3.7.

The dissociation constant of the enzyme·MgATP complex which participates in the synergistic coupling was determined on the basis of eq 5. The Mg^{2+} dependence is sigmoidal (Figure 4). The limits are $K_{MgATP}(max) = 1.4$ mM and $K_{MgATP}(min) = 0.2$ mM. The Mg^{2+} concentration at $(K_{MgATP}(max) - K_{MgATP}(min))/2$ is 4 mM. The value of the Hill constant is determined to be 3.6 (Figure 4, inset).

Effect of Mg^{2+} on the Dissociation Constants of the Enzyme·L-Phenylalanine·MgATP Complex and on the Rate of Synthesis of the Enzyme·Phenylalanyladenylate. In a first approach, the enzyme·L-phenylalanine·MgATP complex was studied by the replacement of MgATP by MgAPCPP, which cannot react with L-phenylalanine because of the substitution of oxygen by a methylene group. It was found that the dissociation constant for L-phenylalanine was not affected in the presence of 1–10 mM of the analoque at different (1–10 mM) concentrations of $MgCl_2$. However, the analogue appears to be a fairly poor substitute since the coupling between the binding of MgAPCPP and of L-phenylalaninol to the enzyme is weak ($s = 5$–10 compared with $s = 390$ in the case of MgATP).

The dissociation constants for L-phenylalanine and MgATP in the enzyme·L-phenylalanine·MgATP complex were determined in the form of the Michaelis–Menten constants of the synthesis of the enzyme·phenylalanyladenylate complex. Measurements were conducted at various concentrations of $MgCl_2$. The technique was to follow the time dependence of the decrease in fluorescence intensity in the presence of TNS (see Materials and Methods).

In the absence of $tRNA^{Phe}$, phenylalanyl-tRNA synthetase and one of the substrates were mixed with the other substrate in a stopped-flow apparatus. The results were the same whether MgATP or phenylalanine was incubated with the enzyme. The reaction mixture contained TNS, and a first-order reaction (up to 90% completion of the reaction) was observed as a decrease of the fluorescence intensity of the dye. As argued in the Discussion, the reaction is attributed to the formation of the enzyme·phenylalanyladenylate complex. The rate constant of the reaction was found to depend on the concentration of MgATP, L-phenylalanine, and Mg^{2+} as will be described.

In the first experiments, the concentration of MgATP was varied at either 1 mM or 10 mM $MgCl_2$ (Figure 5). It is seen that the Michaelis–Menten constant, $K_{m(MgATP)}$, is the source of the Mg^{2+} dependence. An interference by pyrophosphorolysis is ruled out by the presence of inorganic pyrophosphatase. The measurements were performed at 2.3 μM L-phenylalanine, at which only 5–10% of the enzyme was bound to the amino acid (assuming a dissociation constant of 20–35 μM; Bartmann et al., 1975a). Measurements were repeated at 46 μM L-phenylalanine, where 60–70% of the enzyme should be bound to L-phenylalanine. In response, the values of k_{obsd} increased as is expected on the basis of eq 1. The rate constants $k_{obsd(max)}$ at saturating [MgATP] were used to estimate $K_{m(Phe)} = 52 \pm 20$ μM at 1 mM Mg^{2+} and 94 ± 40 μM at 10 mM Mg^{2+}. The values are not definitely higher than the value 20–35 μM for the dissociation constant of the binary complex. However, together with the values of $K_{m(MgATP)}$ that are shifted from 2.9 to 5 mM (1 mM Mg^{2+}) and from 0.6 to 1.1 mM (10 mM Mg^{2+}) when [Phe] increases from 2.3 to 46 μM, they might indicate antagonistic binding of L-phenylalanine and MgATP.

The experiment in Figure 5 indicates that the Mg^{2+} dependence is expressed by the values of $K_{m(MgATP)}$. The study was completed by measuring k_{obsd} at conditions of 0.1 mM MgATP and varying concentrations of $MgCl_2$, where the system was sensitive because of $k_{obsd} \sim [MgATP]/K_{m(MgATP)}$ at $[MgATP] < K_{m(MgATP)}$ (eq 1). The values of k_{obsd} are given with reference to k_{obsd} (10 mM $MgCl_2$) for practical reasons and are plotted in Figure 6A. In the k_{obsd} vs. $k_{obsd}/[Mg^{2+}]$ version (Eadie, 1942), the points were fitted by a linear relation with $K_{m(Mg^{2+})} = 4 \pm 1$ mM.

In the presence of $tRNA^{Phe}$, one of the syringes contained MgATP and phenylalanyl-tRNA synthetase and the other

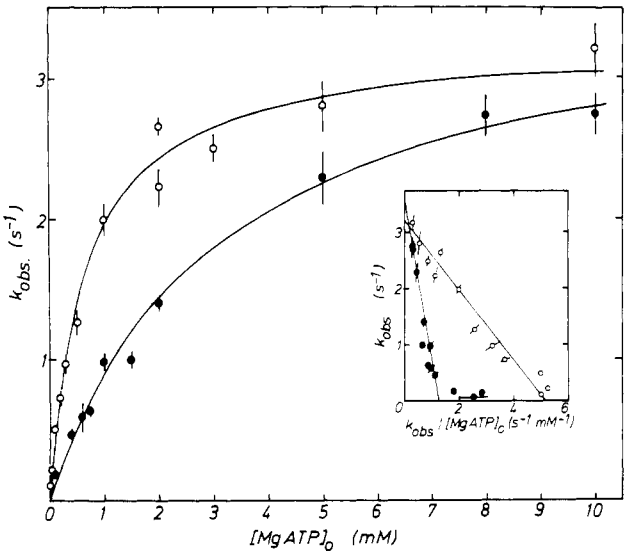

FIGURE 5: Synthesis of phenylalanyladenylate in the absence of tRNA. The time-dependent synthesis of the enzyme·phenylalanyladenylate complex is followed by the decrease in fluorescence intensity in the presence of TNS. Values of k_{obsd} are determined from first-order plots at varying concentrations of MgATP. They are plotted according to Eadie (1942) in the figure inset. Error bars refer to averaged deviations. Conditions are 50 mM Tris-HCl (pH 7.5 and 25 °C), 0.1 mM EDTA, 0.2 mM dithioerythritol, 2 μM TNS, 2.3 μM L-phenylalanine, 150 nM synthetase, and 10 μg/mL inorganic pyrophosphatase. Concentrations of Mg^{2+} are 1 mM (●) and 10 mM (○).

L-phenylalanine. Concentrations of TNS and $MgCl_2$ were identical in both syringes. MgATP and L-phenylalanine could be interchanged without affecting the kinetics. Furthermore, identical results were obtained when MgATP, L-phenylalanine plus $tRNA^{Phe}$ were mixed with the solution of the synthetase. The kinetics were very similar at 1 mM $MgCl_2$ with those where $tRNA^{Phe}$ was absent. But they consisted of two, well-separated phases, one in the 50–500-ms and one in the $\gtrsim$ 10-s range, where $[Mg^{2+}]$ was 10 mM. The rapid decrease constituted 50–60% of the overall decrease observed at equilibrium. It was assigned to the formation of the synthetase·phenylalanyladenylate because of the following reasons. (1) The reaction was not seen when preformed enzyme·adenylate complex was mixed with the $tRNA^{Phe}$. (2) The amplitude of the second reaction became less than 8% when the Mg^{2+} concentration was lowered from 10 mM to 1 mM $MgCl_2$. At this concentration, phenylalanyladenylate has been shown to be the only species contributing to the fluorescence decrease (Bartmann et al., 1975a). (3) The time scale was that of the reaction seen in the absence of $tRNA^{Phe}$.

The slow decrease in fluorescence intensity during the second phase is attributed to the aminoacylation of $tRNA^{Phe}$. The reasons are as follows. (1) The kinetics are consistent with steady-state aminoacylation, where the synthesis of Phe-$tRNA^{Phe}$ is followed radioactively. The steady-state rate constant has been determined to be 3 s^{-1} (Holler, 1976). At 0.094 μM synthetase and 0.054 μM $tRNA^{Phe}$, the fluorescence decreases with a first-order rate constant of 1.8 ± 0.2 s^{-1}, at 0.58 μM synthetase and 0.54 μM $tRNA^{Phe}$ with a rate constant of 2.0 ± 0.2 s^{-1}. (2) The kinetics are found to be sensitive to a variation of the concentration of MgATP. The dependence is hyperbolical and follows a K_m value of 0.25 ± 0.05 mM. The value is compatible with the K_m of 0.17 mM reported for the steady-state kinetics of the aminoacylation (Holler & Kosakowski, 1973). (3) The overall change in fluorescence intensity of the slow reaction follows a saturation dependence when $[tRNA^{Phe}]$ is varied between 0.01 and 1.4 μM (not shown). The tangents to the titration curve at low and high $[tRNA^{Phe}]$ (for details, see Bartmann et al., 1975b) intersect at 0.1 μM. This value compares with the concentration of 0.1 μM enzyme held constant. The 1:1 stoichiometry is attributed to the formation of an enzyme·Phe-$tRNA^{Phe}$ complex as has been described for mixtures of enzyme and Phe-$tRNA^{Phe}$ alone (Holler, 1976).

The rate constant of the synthesis of the enzyme·adenylate complex (Table IV) was measured as a function of [MgATP] in the presence of either 1 mM or 10 mM $MgCl_2$ (Figure 7). Contrary to the experiments in the absence of $tRNA^{Phe}$ (Figure 5), both the parameters $K_{m(MgATP)}$ and $k_{obsd(max)}$ are affected here. The dual dependence expresses itself as a sigmoidal function when k_{obsd} is measured as a function of $[Mg^{2+}]$ at fixed amounts of substrates (Figure 6B). The Hill constant is 3.5, and $[Mg^{2+}]$ at half-maximum rate is 3.6 mM.

In another set of experiments, [Phe] was varied between 2.3 and 100 μM. The dependence of k_{obsd} as a function of [L-phenylalanine] gave rise to $K_{m(Phe)}$ = 40 ± 7 μM as computed from an Eadie (1942) plot (not shown). The value is consistent with the value of the dissociation constant of the binary enzyme·L-phenylalanine complex (20–35 μM; Bartmann et al., 1975a) and at variance with the higher $K_{m(Ile)}$ values in the absence of $tRNA^{Phe}$. Because of eq 1, $k_{obsd(max)} = k_f$-

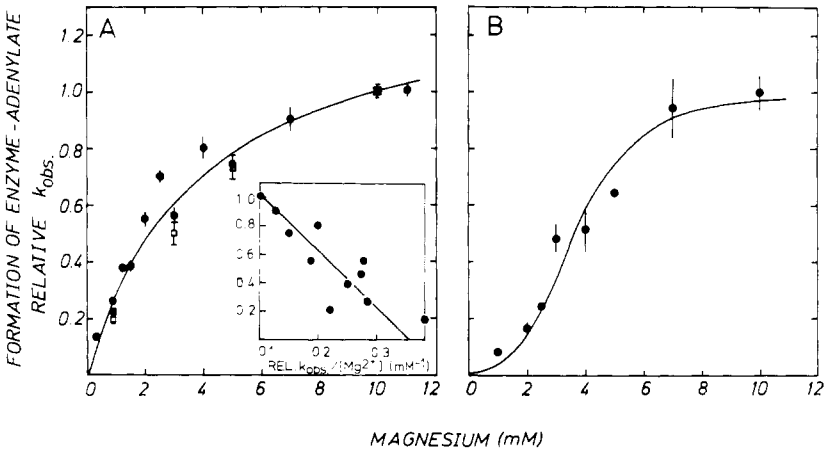

FIGURE 6: Rate of synthesis of phenylalanyladenylate as a function of Mg^{2+}. Conditions are 50 mM Tris-HCl buffer, pH 7.5 (●), or 10 mM potassium phosphate buffer, pH 7.5 (□), 2.3 μM L-phenylalanine, 0.1 mM MgATP, 2 μM TNS, 0.15 μM synthetase, 0.1 mM EDTA, and 0.2 mM dithioerythritol. Temperature was 24 ± 0.1 °C. (A) $tRNA^{Phe}$ is absent. Results are plotted according to Eadie (1942) in the inset. The drawn curve is obtained for $K_{m(Mg^{2+})}$ = 4 mM. (B) $[tRNA^{Phe}]$ is 0.54 μM and [L-phenylalanine] = 90 μM. The experimental points can be fitted by the Hill equation $k_{obsd}(rel) = [Mg^{2+}]^{3.5}/([Mg^{2+}]^{3.5} + 3.6 \times 10^{-3})$.

Table IV: Kinetic Parameters of the Synthesis and the Pyrophosphorolysis of the Enzyme·Phenylalanyladenylate Complex[a]

Mg^{2+} (mM)	$tRNA^{Phe}$ (μM)	Phe (μM)	MgATP (mM)	$K_{m(Phe)}$ (μM)	$K_{m(MgATP)}$ (mM)	$K_{m(MgPP_i)}$ (mM)	$k_{obsd(max)}$ (s^{-1})
1		2.3	var	52 ± 20	2.9 ± 0.3		3.6 ± 0.5
1		46	var		5 ± 1		40 ± 5
10		2.3	var	94 ± 40	0.6 ± 0.07		3.2 ± 0.3
10		46	var		1.1 ± 0.1		44 ± 5
1	0.54	19	var		1.5 ± 0.2		7.0 ± 0.4
10	0.54	19	var		0.54 ± 0.09		27 ± 2
10	0.54	var	0.5	40 ± 7			40 ± 5
1		2.3	0.2			0.3 ± 0.005	60 ± 5
10		2.3	0.2			0.060 ± 0.005	60 ± 5
1	0.63	11.5	0.5			0.57 ± 0.07	105 ± 15
10	0.54	2.3	0.2			0.14 ± 0.02	90 ± 10

[a] The parameters have been obtained from experiments in Figures 5–8 and those described in the text. In all experiments, except where $[MgPP_i]$ is varied, the concentration of pyrophosphate is negligible because of its hydrolysis by inorganic pyrophosphatase. The values $K_{m(MgPP_i)}$ have been corrected for the formation of Mg_2PP_i as is described in the text. The values $K_{m(Phe)}$ in the absence of tRNA have been calculated on the basis of eq 1 and the values of $k_{obsd(max)}$ for 2.3 μM and 46 μM, respectively.

Table V: Kinetic and Equilibrium Constants of the Synthesis of Enzyme·Phenylalanyladenylate[a]

Mg^{2+} (mM)	Phe (μM)	$tRNA^{Phe}$ (μM)	k_f (s^{-1})	k_b (s^{-1})	k_f/k_b	K_{eq} (μM)
1	2.3		86 ± 30	72 ± 8	1.2 ± 0.4	420 ± 220
	46					720 ± 400
10	2.3		134 ± 50	60 ± 5	2.2 ± 0.9	430 ± 260
	46					780 ± 470
1	19	0.54	22 ± 4	105 ± 15	0.21 ± 0.05	500 ± 170
10	19	0.54	84 ± 14	90 ± 10	0.93 ± 0.19	170 ± 50
	∞	0.54	83 ± 18		0.92 ± 0.22	170 ± 60

[a] Rate constants k_f and k_b of the amino acid activation reaction, eq 2, are computed on the basis of eq 1. The values of the Michaelis–Menten constants, of $k_{obsd(max)}$ and of the substrate concentrations in Table IV are used. The equilibrium constant K_{eq} is calculated on the basis of eq 8. Conditions are 50 mM Tris-HCl (pH 7.5), 0.1 mM EDTA, 0.2 mM dithioerythritol, and 25 °C.

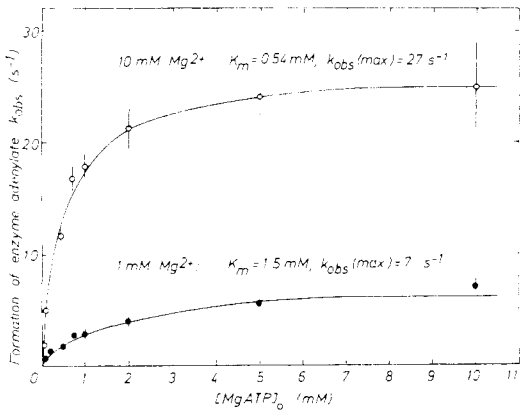

FIGURE 7: Synthesis of phenylalanyladenylate in the presence of $tRNA^{Phe}$. Experiments are the same as under Figure 5 except that the reaction mixture contained 19 μM L-phenylalanine, 0.54 μM $tRNA^{Phe}$, 0.083 μM enzyme, 4.5 μM TNS, and either 1 mM $MgCl_2$ (●) or 10 mM (○) and the other components under Figure 5.

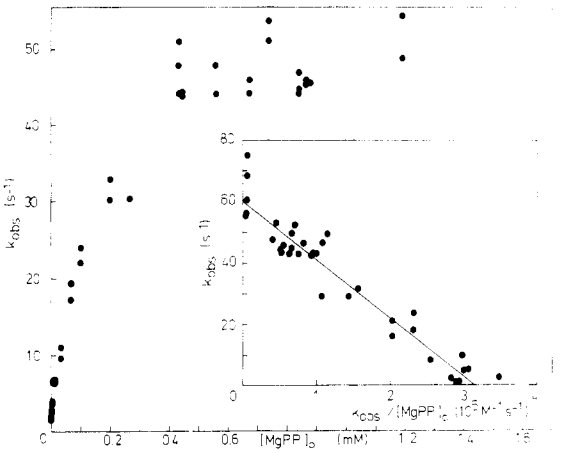

FIGURE 8: Pyrophosphorolysis of phenylalanyladenylate in the absence of $tRNA^{Phe}$. The reaction is initiated in a stopped-flow apparatus by mixing a solution containing the enzyme·phenylalanyladenylate complex with a solution of magnesium pyrophosphate. The adenylate complex is prepared by preincubating 0.05–0.17 μM phenylalanyl-tRNA synthetase, 0.2–0.4 mM MgATP, 2.3–4.6 μM L-phenylalanine, and (0.2–1 μg/mL) inorganic pyrophosphatase for 5 min at 25 °C in one of the syringes. The substrates are supplied in the same concentrations to the other syringe together with $MgPP_i$. Other conditions were 50 mM Tris-HCl buffer (pH 7.5 at 25 °C), 10 mM $MgCl_2$, 4 μM TNS, 0.1 mM EDTA, and 0.2 mM dithioerythritol. The values of k_{obsd} have been corrected with 0.5 s^{-1} for the resynthesis of the adenylate on the basis of eq 1.

$[MgATP]/(K_{MgATP} + [MgATP])$ when [Phe] is varied and [MgATP] = 0.5 mM is held constant. By substituting the values of MgATP and $K_{m(MgATP)}$ = 0.54 mM (at 10 mM $MgCl_2$, 0.54 μM $tRNA^{Phe}$), a value of k_f = 83 s^{-1} was obtained. This value is the same as that obtained from the data of Figure 7 when [MgATP] was varied and [Phe] held constant (see Table V).

Effect of Mg^{2+} on the Kinetics of Pyrophosphorolysis of the Enzyme·Phenylalanyladenylate Complex. Pyrophosphorolysis was initiated by a rapid mixing of a 5 min (25 °C) preincubated mixture of phenylalanyl-tRNA synthetase, L-phenylalanine, MgATP and inorganic pyrophosphatase with a solution containing $MgPP_i$. The concentration of the pyrophosphatase (0.2–1 μg/mL) is sufficient to hydrolyze PP_i during incubation with the synthetase but not to appreciably affect the concentration of $MgPP_i$ during the short time of the kinetic measurement. Pyrophosphorolysis was followed by an increase in the fluorescence intensity of TNS. The reactions were first order in both the presence and the absence of $tRNA^{Phe}$. Controls with L-phenylalanine or MgATP alone or in the presence of $tRNA^{Phe}$ did not exhibit the time-dependent fluorescence change. Simple dilution of the incubation mixture with buffer instead of the $MgPP_i$ solution also did not give rise to the observed reactions. The sign and, in the absence of the

tRNA, the magnitude of the reaction amplitude are in accord with the reaction of the adenylate and $MgPP_i$ to give L-phenylalanine and MgATP. At low concentrations, these products dissociate from the enzyme, allowing the reassociation of TNS and the reappearance of the fluorescence.

When plotted as a function of [$MgPP_i$] ($tRNA^{Phe}$ absent), the observed rate constants followed a simple hyperbolic curve (Figure 8). In this plot, the tendency of pyrophosphate to form a dimagnesium salt has been taken into account by multiplying the observed Michaelis–Menten constant, $K_{m(MgPP_i)}$, with the factor 0.3 at 10 mM $MgCl_2$ (and 0.9 at 1 mM $MgCl_2$). The factors were calculated from the dissociation constant of 4.5 mM which pertains to $Mg_2PP_i \rightleftharpoons MgPP_i + Mg^{2+}$ (Lambert & Watters, 1957) and with the assumption that Mg_2PP_i cannot associate with the synthetase (as shown for isoleucyl-tRNA synthetase by Cole & Schimmel (1970)). The values of $K_{m(MgPP_i)}$ are found to decrease as the concentration of Mg^{2+} increases (Table IV). The value of $k_{obsd(max)}$ is the same for 1 mM and 10 mM Mg^{2+}. The effect of $tRNA^{Phe}$ is to increase the values of both $K_{m(MgPP_i)}$ and $k_{obsd(max)}$.

The overall increase in fluorescence intensity varied as a function of [Mg^{2+}] when $tRNA^{Phe}$ was present. It was the same for the presence and absence of $tRNA^{Phe}$ at 1 mM Mg^{2+} but up to 40% smaller at 10 mM Mg^{2+}. This difference could be overcome at high [TNS] (>40 μM). It is attributed to the interaction of Phe-$tRNA^{Phe}$ with enzyme·TNS (Holler, 1976). Since the effect of increasing concentrations of $MgCl_2$ from 1 to 10 mM invariably causes an increase of the ionic strength, controls were added to recognize unspecific effects. Of the salts NaCl (0.5 M), $(NH_4)_2SO_4$ (0.032 M), KF (0.025 M), and KCl (0.4 M) all were moderately inhibitory for the rate of synthesis of the adenylate and of the pyrophosphorolysis (conditions of Figure 5 at 0.1 mM MgATP for the synthesis and of Figure 8 at 0.03 mM $MgPP_i$ for the pyrophosphorolysis). Rate constants decreased two- to threefold. Since this effect has the opposite sign, it cannot contribute to the observed rate acceleration by Mg^{2+}. Furthermore, a specific effect by the Tris-HCl buffer can be ruled out in the case of the adenylate synthesis since the results for phosphate buffer are comparable (Figure 6A).

Discussion

Phenylalanyl-tRNA synthetase of *E. coli* consists of subunits with molecular weights 39000 (α) and 94000 (β). The quaternary structure is of the $(\alpha\beta)_2$-type "pseudo-dimeric" structure (Hanke et al., 1974; Fayat et al., 1974). The enzyme has two active sites, which are occupied in an anticooperative fashion by each, L-phenylalanine and $tRNA^{Phe}$ (Bartmann et al., 1975a). Anticooperative binding between unlike substrate molecules has been reported for L-phenylalanine and $tRNA^{Phe}$ (Bartmann et al., 1975a) and between $tRNA^{Phe}$ and Phe-$tRNA^{Phe}$ (Güntner & Holler, 1979). Mg^{2+} has been shown to bind directly to the enzyme affecting reactivation kinetics after pH 2 dissociation into subunits (Hanke et al., 1975) and to be an activator of the catalytic aminoacylation of $tRNA^{Phe}$ (Bartmann et al., 1975a; Holler, 1976). The other details of the effects of Mg^{2+} are summarized here.

Binding of Mg^{2+} to Phenylalanyl-tRNA Synthetase. Neither the intrinsic protein fluorescence nor the circular dichroism reveals whether Mg^{2+} interacts with the enzyme. Gross conformational changes of the protein backbone would be excluded for this reason. Binding is visible in the presence of TNS. The observed change in fluorescence intensity is caused by an increase of the affinity to form the fluorescent enzyme·TNS complex as the value of the dissociation constant varies from 0.069 to 0.02 mM in the presence of 0–12.6 mM Mg^{2+} (Holler & Kosakowski, 1973). Rapid mixing experiments show that this effect occurs faster than does the association of TNS to form more complex. The increase in fluorescence intensity follows a biphasic concentration dependence (Figure 1 and Table I), indicating two classes of Mg^{2+} binding sites. Whether the sites are nonequivalent in the free enzyme or whether their occupancy follows negative cooperativity remains to be investigated. The binding at the low affinity sites causes a larger effect than that at the high affinity sites. The larger effect is paralleled by the activation of both the adenylate synthesis (Figures 5–7, Table IV) and the tRNA-aminoacylation (Bartmann et al., 1975a; Holler, 1976) and also by a strengthening of the synergistic coupling (Figure 3). Biphasic concentration dependencies have been measured for the binding of Mn^{2+} and spermine·4HCl. These cations inhibit catalysis at concentrations at which they occupy the low affinity sites (Holler et al., 1975a; E. Holler, to be published).

How Many Mg^{2+} Ions Interact with the Enzyme? The strengthening of the synergistic coupling and the activation of the catalytic reactions follow, in all but one case (Figure 6A), a sigmoidal Mg^{2+} concentration dependence (Figure 3–5 and 7; Bartmann et al., 1975a). Hill constants are of the order 3.5–3.7 and could be related to the cooperative association of the enzyme and at least four Mg^{2+} ions. Another explanation, which takes into account the hyperbolic concentration dependencies in Figures 1 and 6A, is that the observed Hill constants are the products of an interplay of more than one Mg^{2+}-dependent elementary reaction. An example is the Mg^{2+} dependence of k_{obsd} of the adenylate synthesis in the presence of $tRNA^{Phe}$ (Figure 6B). Here, both the parameters $K_{m(MgATP)}$ and $k_{obsd(max)}$ are Mg^{2+} dependent (Figure 7 and Table IV). The dependence of k_{obsd} can be formulated by eq 7 where the

$$k_{obsd} = k_{max\infty}\frac{[Mg^{2+}]^x}{K_{1/2} + [Mg^{2+}]^x}\,\frac{[MgATP]}{K_{m(MTP)}\dfrac{[Mg^{2+}]^y}{K_{1/2} + [Mg^{2+}]^y} + [MgATP]} \quad (7)$$

corresponding new Hill constants x and y could be less than 3.5, indicating cooperativity for less than four Mg^{2+} ions. The equation is obtained from eq 1, including the abbreviation of $k_{max\infty}$ for $k_f[Phe]/(K_{m(MgATP)} + [Phe])$ when Mg^{2+} is saturating and $K_{m(MgATP)}$ for the Michaelis–Menten constant under the same condition. It is also possible that, in those non-sigmoidal cases, the cooperativity is lost because, for some unknown reason, the association of the Mg^{2+} ions is uncoupled. Work is underway to clarify that point.

Anticooperative Binding. We have previously determined the dissociation constant of the enzyme·MgATP complex to be 0.6 mM at 15 mM Mg^{2+} by the same technique as is used here (Kosakowski & Holler, 1973). This, and the observation of only a monophasic titration curve, is at variance with the results in Figure 2 and Table II. The reason for the previous value is the comparably narrow range of 0.3–2 mM MgATP, over which the fluorescence change was fitted by a hyperbolic saturation curve. The results of a titration with 0.1–10 mM MgATP at 2 mM Mg^{2+} (Table II) were again ascribed to a monophasic concentration dependence. If, as is the case for the titration at 10 mM Mg^{2+} (Figure 2), the value $\Delta F_{\infty(1)}/F_0$ of the high affinity sites is only 25% of the total decrease of the fluorescence intensity, then $\Delta F_{\infty(1)}/F_0$ at 2 mM Mg^{2+} should be less than 0.1 and would be difficult to detect. To summarize, the fluorometric method might not be adequate

to indicate biphasic binding under all conditions. A reliable method would be equilibrium dialysis. However, the method suffers from the requirement of millimolar concentrations of the enzyme to form measurable amounts of E·$(MgATP)_2$ complexes.

Under the assumption of rapid preequilibrium, the values of the Michaelis–Menten constants for the adenylate synthesis can be compared with the values of the dissociation constants obtained under noncatalytical conditions. Inspection of Figures 5 and 7 reveals monophasic functions of k_{obsd} as [MgATP] is varied. If the affinity of the substrate to bind to the first and second active site is not the same, one of these must display a catalytic activity that is hardly detectable.

As in the case of Mg^{2+} in Figure 1 and with MgATP in Figure 2, biphasic binding curves have been obtained by equilibrium dialysis for L-phenylalanine and by equilibrium gel filtration for $tRNA^{Phe}$ (Bartmann et al., 1975a). Two molecules of the same substrate were bound to the enzyme at saturating conditions. Because the enzyme has been found by chemical (Hanke et al., 1974, 1975), by immunochemical (Hennecke et al., 1977b), and by genetical analysis (Comer & Böck, 1976; Hennecke et al., 1977a) to consist of only single kinds of α and β subunits, it is highly probable that the properties of the active sites are identical in the unliganded enzyme and that the binding of the substrates and of Mg^{2+} follows an anticooperative fashion.

Coupling Phenomena. Increasing [Mg^{2+}] affects the binding of TNS (Holler & Kosakowski, 1973), of L-phenylalaninol (Table III), of MgATP (Figures 4 and 5), and of $MgPP_i$ (Table IV) but not of L-phenylalanine (Bartmann et al., 1975a). The value of the dissociation constant of the enzyme·L-phenylalaninol complex increases, while the values of the Michaelis–Menten constants for MgATP and $MgPP_i$ of the adenylate synthesis and the pyrophosphorolysis, respectively, decrease. The source of the coupling appears to be an increased positive charge at the active site(s) when Mg^{2+} is bound. Such a change could generate a repulsion of the positively charged L-phenylalaninol and an attraction of the negatively charged MgATP and $MgPP_i$ but would have no effect in the case of the zwitterionic L-phenylalanine. The coupling does not occur with the unliganded enzyme·MgATP complexes as is concluded from the similar values of the dissociation constants 6 mM (Kosakowski & Holler, 1973), 5 mM, and 9.1 mM (Table II) at zero, 2 mM, and 10 mM Mg^{2+}, respectively. A prerequisite for the coupling seems to be the additional binding of either L-phenylalaninol or L-phenylalanine.

A synergistic coupling has been reported for the binding of L-phenylalaninol and MgATP (Kosakowski & Holler, 1973). At zero [Mg^{2+}], the coupling is not detected unless ATP is substituted by adenosine (Kosakowski & Holler, 1973). At 1 mM Mg^{2+}, the coupling constant for MgATP (s = 15) is comparable with the coupling constant for adenosine (s = 19) (Figure 3) and the binding of MgATP to the high affinity site is indicated (Figure 4). As [Mg^{2+}] becomes higher, the values of the coupling constant and of the dissociation constant for MgATP increase in a sigmoidal fashion (Figures 3 and 4). At 10 mM Mg^{2+}, the coupling constant is s = 290 and the dissociation constant 1.4 mM. Our speculation is that the coupling observed at 1 mM Mg^{2+} reflects the synergistic reaction at a single active site, while the coupling at 10 mM Mg^{2+} involves a simultaneous synergistic reaction at both active sites. For instance, binding of L-phenylalaninol to a single site couples at 10 mM Mg^{2+} with the complex formation of MgATP at the two active sites simultaneously. This explains why the dissociation constant for MgATP assumes higher values at higher [Mg^{2+}] (Figure 4). Moreover, the synergistic coupling constant, s_{max}, is expected on this basis to be the product of the coupling constants at single active sites, s_{max}, = $s_{min}s_{min}$ = 15 × 15 = 225. The observed value is s_{max} = 290 (Figure 3). Such a coupling between active sites could be interesting with respect to half-of-the-sites reactivity, which has been discussed for phenylalanyl-tRNA synthetase of yeast (Fasiolo et al., 1977).

Kinetics and Thermodynamics of the Adenylate Synthesis. The interpretation that the observed decrease in fluorescence intensity is related to the synthesis of enzyme-bound adenylate is based on the following arguments. (1) Phenylalaninol adenosine monophosphate, a structural analogue of phenylalanyladenylate (Cassio et al., 1967), is a competitive inhibitor with respect to L-phenylalanine (Santi et al., 1971), a fact predicting the displacement of TNS by the adenylate. (2) When PP_i is removed by inorganic pyrophosphatase, the decrease in fluorescence intensity is almost maximal at less than 1 μM Phe and less than 0.1 mM MgATP, because the adenylate is synthetized, but is almost zero under noncatalytic conditions. (3) Previous kinetic results obtained by the fluorescence technique are in agreement with results from radioactive measurements (Bartmann et al., 1975a; Mulivor & Rappaport, 1973).

Rate constants k_f were computed from the results in Table IV on the basis of eq 1, assuming saturation by both MgATP and Phe. They are summarized in Table V. The rate constant k_b for the pyrophosphorolysis was taken to be equal to $k_{obsd(max)}$. The equilibrium constant k_f/k_b is of the order of unity in almost all cases. In the presence of $tRNA^{Phe}$ and 1 mM Mg^{2+}, the equilibrium constant is definitively smaller (Table V). Previously determined values at 1 mM Mg^{2+} in the absence of $tRNA^{Phe}$ were 0.3–0.5 (Bartmann et al., 1975a). An equilibrium constant K_{eq} has been defined (Holler & Calvin, 1972) as shown in eq 8. Values of K_{eq} have been computed

$$K_{eq} = \frac{[E][MgATP][Phe]}{[E{\cdot}Phe{\sim}AMP][MgPP_i]} = \frac{k_b}{k_f}\frac{K_{m(Phe)}K_{m(MgATP)}}{K_{m(MgPP_i)}} \quad (8)$$

by using the K_m values and rate constants in Tables IV and V. They are found to be independent of [Mg^{2+}] except when $tRNA^{Phe}$ is present (Table V). In this case, the enzyme·adenylate complex forms somewhat easier at 10 mM Mg^{2+} than at 1 mM. A comparison with previous work indicates that the present values are higher by factors 3–13 (Bartmann et al., 1975a; Mulivor & Rappaport, 1973). The disagreement is not subject of an error fluctuation but presumably a consequence of different experimental approaches. Conditions of Bartmann et al. (1975a) were 2 μM Phe and 0.1 mM MgATP. Their computations were based on the erroneous value of 0.6 mM for the dissociation constant of the enzyme·MgATP complex and they were not aware of the antagonistic binding of Phe and MgATP. One of their conditions is the presence of $MgPP_i$ as is the case in the ATP–PP_i exchange measurements of Mulivor & Rappaport (1973). If $MgPP_i$ binds to the active sites in an anticooperative fashion and if the binding affects the complex formation of the other substrates, different results for K_{eq} are likely to be obtained.

It can be seen from Tables IV and V that $tRNA^{Phe}$ modulates the values of $K_{m(MgATP)}$, $K_{m(MgPP_i)}$, k_f (at 1 mM Mg^{2+}), and K_{eq}. The modulation is at its maximum a factor of 5. It expresses a coupling between the binding of $tRNA^{Phe}$, MgATP, or $MgPP_i$. Santi et al. (1971) observed a decrease of the ATP-PP_i exchange rate in the presence of $tRNA^{Phe}$ and came to a similar conclusion. The difference between the K_m

values for Phe and MgATP of the adenylate synthesis and the steady-state aminoacylation of tRNA (Santi et al., 1971; Holler & Kosakowski, 1973) can probably be explained kinetically as has similarly been discussed in the case of chymotrypsin (Gutfreund & Sturtevant, 1956; Hess et al., 1970) and of phenylalanyl-tRNA synthetase (Holler & Kosakowski, 1973).

Other Aminoacyl-tRNA Synthetases. It has been generally accepted, and has been demonstrated for the L-isoleucine-specific and the L-arginine-specific enzymes of *E. coli*, that MgATP is the active form of ATP during catalysis by aminoacyl-tRNA synthetases (Cole & Schimmel, 1970; Craine & Peterkofsky, 1976). Loftfield & Eigner (1969) have postulated that a second metal ion is required in the isoleucine-specific system of *E. coli*. The direct uptake of Mg^{2+} in the millimolar concentration range by the same enzyme has been demonstrated by Holler (1973). A requirement for a second Mg^{2+} has been derived from catalytic steady-state kinetics in the case of arginyl-tRNA synthetase by Craine & Peterkofsky (1976). The action of magnesium during the transfer of L-phenylalanine from AMP to $tRNA^{Phe}$ by phenylalanyl-tRNA synthetase of yeast has been attributed to the stabilization of a native conformation of $tRNA^{Phe}$ (Robinson & Zimmerman, 1971). Von der Haar (1976) has related biphasic steady-state kinetics of aminoacylation by the same enzyme to the existence of two forms of the synthetase that are interconvertable in the presence of magnesium. Hyafil & Blanquet (1977) observe competition between Mg^{2+} and L-methioninol for methionyl-tRNA synthetase of *E. coli* in the millimolar concentration range of the metal ion. It is suggested that the cation could be involved in the opening of a preexisting ion pair. Such a pair has been postulated to interact with the amino acid and ATP (Holler et al., 1975).

Conclusion

The catalytically significant dissociation constants of MgATP and $MgPP_i$ and their Michaelis–Menten constants vary considerably as a function of the reaction condition and of the concentration of Mg^{2+}. The effects of Mg^{2+} seem to arise from an interaction between 2 or more Mg^{2+} and the enzyme by a modulation of the coupling between the active sites.

Acknowledgments

We thank Dr. R. Leitsmann of the Chemische Fabrik Heyden for supplying facilities which enabled us to carry out a large-scale preparation of hydroxylapatite. The technical assistance of G. Schwarze is gratefully acknowledged.

References

Bartmann, P., Hanke, T., & Holler, E. (1975a) *Biochemistry 14*, 4777.

Bartmann, P., Hanke, T., & Holler, E. (1975b) *J. Biol. Chem. 250*, 7668.

Blanquet, S., Fayat, G., & Waller, J.-P. (1975) *J. Mol. Biol. 94*, 1.

Cassio, D., Lemoine, F., Waller, J.-P., Sandrin, E., & Boissanas, R. A. (1967) *Biochemistry 6*, 827.

Cole, F. X., & Schimmel, P. R. (1970) *Biochemistry 9*, 3143.

Comer, M. M., & Böck, A. (1976) *J. Bacteriol. 127*, 923.

Craine, J. E., & Peterkofsky, A. (1976) *J. Biol. Chem. 251*, 241.

Eadie, G. S. (1942) *J. Biol. Chem. 146*, 85.

Fasiolo, F., Ebel, J.-P., & Lazdunski, M. (1977) *Eur. J. Biochem. 73*, 7.

Fayat, G., Blanquet, S., Dessen, P., Batelier, G., & Waller, J.-P. (1974) *Biochimie 56*, 35.

Goody, R. S., & Eckstein, F. (1971) *J. Am. Chem. Soc. 93*, 6252.

Güntner, C., & Holler, E. (1979) *Biochemistry 18*, 2028.

Gutfreund, H., & Sturtevant, J. M. (1956) *Biochem. J. 63*, 656.

Hanke, T., Bartmann, P., Hennecke, H., Kosakowski, H. M., Jaenicke, R., Holler, E., & Böck, A. (1974) *Eur. J. Biochem. 43*, 601.

Hanke, T., Bartmann, P., & Holler, E. (1975) *Eur. J. Biochem. 56*, 605.

Hennecke, H., Springer, M., & Böck, A. (1977a) *Mol. Gen. Genet. 152*, 205.

Hennecke, H., Walther, I., & Franz, H. (1977b) *Hoppe-Seyler's Z. Physiol. Chem. 358*, 197.

Hess, G. P., McConn, J., Ku, E., & McConkey, G. (1970) *Philos. Trans. R. Soc. London, Ser. B 257*, 89.

Holler, E. (1973) *Biochemistry 12*, 1142.

Holler, E. (1976) *J. Biol. Chem. 251*, 7717.

Holler, E., & Calvin, M. (1972) *Biochemistry 11*, 3741.

Holler, E., & Kosakowski, H. M. (1973) *Biochem. Biophys. Res. Commun. 54*, 1532.

Holler, E., Bennett, E. L., & Calvin, M. (1971) *Biochem. Biophys. Res. Commun. 45*, 409.

Holler, E., Rainey, P., Orme, A., Bennett, E. L., & Calvin, M. (1973) *Biochemistry 12*, 1150.

Holler, E., Hammer-Raber, B., Hanke, T., & Bartmann, P. (1975) *Biochemistry 14*, 2496.

Hyafil, F., & Blanquet, S. (1977) *Eur. J. Biochem. 74*, 481.

Klotz, I. M., & Hunston, D. L. (1971) *Biochemistry 10*, 3065.

Kosakowski, H. M., & Böck, A. (1970) *Eur. J. Biochem. 12*, 67.

Kosakowski, H. M., & Holler, E. (1973) *Eur. J. Biochem. 38*, 274.

Lambert, S. M., & Watters, J. (1957) *J. Am. Chem. Soc. 79*, 5606.

Loftfield, R. B., & Eigner, E. A. (1969) *J. Biol. Chem. 244*, 1746.

Lynch, D. C., & Schimmel, P. R. (1974) *Biochemistry 13*, 1841.

Mulivor, R., & Rappaport, H. P. (1973) *J. Mol. Biol. 76*, 123.

Rainey, P., Hammer-Raber, B., Kula, M.-R., & Holler, E. (1977) *Eur. J. Biochem. 78*, 239.

Robinson, B., & Zimmerman, T. P. (1971) *J. Biol. Chem. 246*, 4664.

Santi, D. V., Daneneberg, P. V., & Satterly, P. (1971) *Biochemistry 10*, 4804.

Von der Haar, F. (1976) *Eur. J. Biochem. 64*, 395.